On the effect of line current width and relative position on the multi-spacecraft curlometer technique

C. Forsyth[*,a], M. Lester[b], A. N. Fazakerley[a], C. J. Owen[a], A. P. Walsh[a]

[a] *UCL Mullard Space Science Laboratory, Holmbury St. Mary, Dorking, Surrey, RH5 6NT, United Kingdom*
[b] *Dept. Physics and Astronomy, University of Leicester, University Road, Leicester, LE1 7RH, United Kingdom*

Abstract

The response of the multi-spacecraft curlometer technique to variations in the size and relative position of infinitely long line currents with radially varying current density is systematically investigated for spacecraft in a regular tetrahedral formation. It is shown that, for line currents with a width less than the spacecraft separation, there is significant variation in the returned current with position of that current within the tetrahedron. For infinitely thin line currents, the curlometer tends to detect approximately 20% of the input current. For increasingly wide line currents there is less variation of the curlometer results with position of the current and the percentage of current magnitude detected increases. When the width of the current system is half the spacecraft separation, the curlometer tends to detect approximately 80% of the input current. These results are discussed in the context of multi-scale, multi-spacecraft missions.

Key words:

1. Introduction

Currents are a critical part of any magnetised plasma environment, with current sheets separating different plasma regimes through magnetic field shears and current sheets, and line currents transporting energy along magnetic field-lines. They are also intrinsically linked to electric and magnetic fields and as

*Corresponding author
Email address: cfo@mssl.ucl.ac.uk (C. Forsyth)

such, may play an important part in the reconnection of magnetic field lines. In particular, the currents appear in two terms of the Generalised Ohm's Law, the Hall term and the anomalous resistivity term, which may be important at different scale sizes. As such, in order to understand fundamental physical processes within plasmas, it is necessary to accurately compare currents detected at different scale sizes.

The curlometer technique (Dunlop et al., 1988) combines magnetic field data from four non-coplanar spacecraft, assuming linear variations of the field between the spacecraft, to determine the dyad $\nabla\mathbf{B}$. An estimate of the curl of the magnetic field within the volume delimited by the spacecraft can be calculated by combining the off-diagonal terms of this dyad. In the absence of high frequency variations in the electric field, Ampére's law states that the curl of the magnetic field is proportional to the current density through the volume, hence from this estimate of $\nabla \times \mathbf{B}$, an estimate of the current density flowing through the spacecraft tetrahedron can be found.

The curlometer technique also allows an estimate of $\nabla \cdot \mathbf{B}$ to be calculated from the diagonal terms in $\nabla\mathbf{B}$. Due to a combination of the non-linear variations of the magnetic field within the spacecraft volume and uncertainties in the measurements of magnetic field values and spacecraft position, the estimated $\nabla \cdot \mathbf{B}$ is almost always non-zero. Given Gauss' Magnetic Field Law ($\nabla \cdot \mathbf{B} = 0$), it is clear that any non-zero estimation of $\nabla \cdot \mathbf{B}$ is indicative of the limitations of the technique, although it is not necessarily indicative of the uncertainty in the estimate of the current density. Robert et al. (1998) showed that there was no one-to-one correlation between the relative error in the current density, $\triangle j/j$, and $|\nabla \cdot \mathbf{B}/\nabla \times \mathbf{B}|$ although statistically the two were similar.

The curlometer technique has been used to investigate physical processes in the magnetosphere using data from the Cluster spacecraft. At a system level, the Cluster spacecraft have been used to measure the magnetopause currents (e.g. Dunlop et al., 2002; Dunlop and Balogh, 2005) and magnetotail current sheet (e.g. Runov et al., 2003, 2005, 2006). Dynamical features such as flux transfer events (Phan et al., 2004) and bursty bulk flows (Forsyth et al., 2008) have also been examined. At a more physical level, the curlometer has been used to compare the Hall and electron pressure tensor terms in the Generalised Ohm's law (Henderson et al., 2006, 2008). For a more complete review of previous work using the curlometer technique see the review paper by Dunlop and Eastwood (2008).

Previous studies have investigated the curlometer's accuracy for a variety of tetrahedron shapes, driven by the fact that, without significant manoeuvring of the spacecraft during an orbit, the shape of a constellation of spacecraft will evolve along that orbit (e.g. Robert and Roux, 1993; Dunlop and Balogh, 1993; Coeur-Joly et al., 1995; Robert et al., 1995, 1998). The majority of these studies suggested various quality parameters based on the shape of the tetrahedron and examined them using the Tsyganenko (1987) magnetic field model. It was noted, however, that local, transient variations in the Earth's magnetic field that were not included in the model could invalidate these quality parameters as the accuracy of the estimates of $\mathbf{j}$ is dependent on both the shape of the spacecraft tetrahedron and the configuration of the magnetic field.

Runov et al. (2005) modelled the response of the curlometer to a Harris-type current sheet (Harris, 1962) in order to determine an appropriate limit for $|\nabla \cdot \mathbf{B}/\nabla \times \mathbf{B}|$ below which the currents returned by the curlometer are valid. They showed that, for the Harris-type current sheets, $|\nabla \cdot \mathbf{B}/\nabla \times \mathbf{B}|$ and $\triangle j/j$ did not vary linearly with changing scale sizes of the current sheet, although both decreased with increasing scale size. $|\nabla \cdot \mathbf{B}/\nabla \times \mathbf{B}|$ appeared to tend towards 0.28 for current systems larger than the spacecraft tetrahedron.

As previous studies are concerned with planar currents, this study concentrates on the effects of the relative scale size of the tetrahedron and a line current, and the effect of the position of the centre of this current system relative to the spacecraft tetrahedron. Although the majority of currents encountered in the magnetosphere will be in current sheets, field-aligned currents associated with features such as bursty bulk flows, flux transfer events and flux ropes may be more filamentary in nature or have a form such that the radial extent is of the same order as the spacecraft separation. In the following sections we will

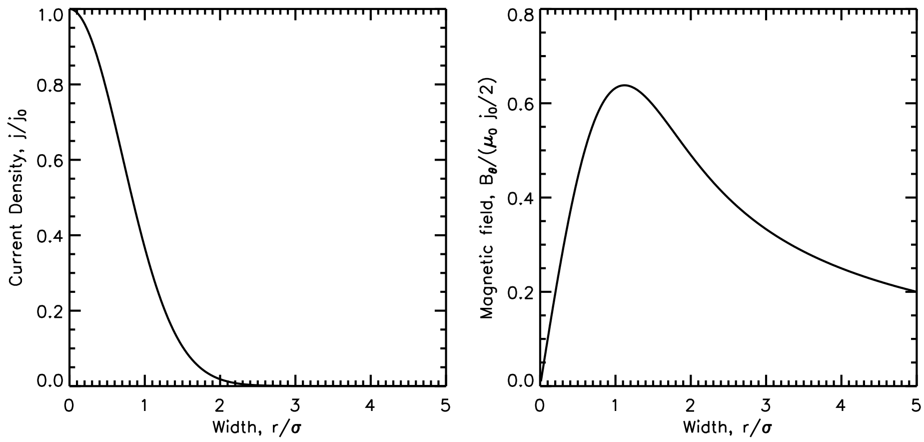

Figure 1: Plots of (a) j_{in}/j_0 and (b) $|B_\theta(r)|$ against radial position in units of the width of the current system, r/σ.

describe the methodology and the model line current system employed, show how the various parameters calculated by the curlometer vary with line current width and location, and discuss the considerations that need to be made when applying the curlometer technique to multi-scale observations and to different current structures.

2. Model set up

The current system employed in this study is an infinitely long current system with a current density distribution of $j_{in}(\mathbf{r}) = j_0 e^{-r^2/\sigma^2}\hat{\mathbf{z}}$ where σ is a constant which we refer to as the width of the current system. The magnetic field from this current system is then given by

$$B_\theta(\mathbf{r}) = K(1 - e^{-r^2/\sigma^2}) + constant \tag{1}$$

where $K = \mu_0 \pi j_0 / 2\pi r$. The form of this current system and the associated magnetic field magnitude are shown in Fig. 1

Given that previous studies have shown that irregular spacecraft tetrahedra have an effect on the results of the curlometer, we distribute our test "spacecraft" in a regular tetrahedron, with three spacecraft in the XY plane and one below

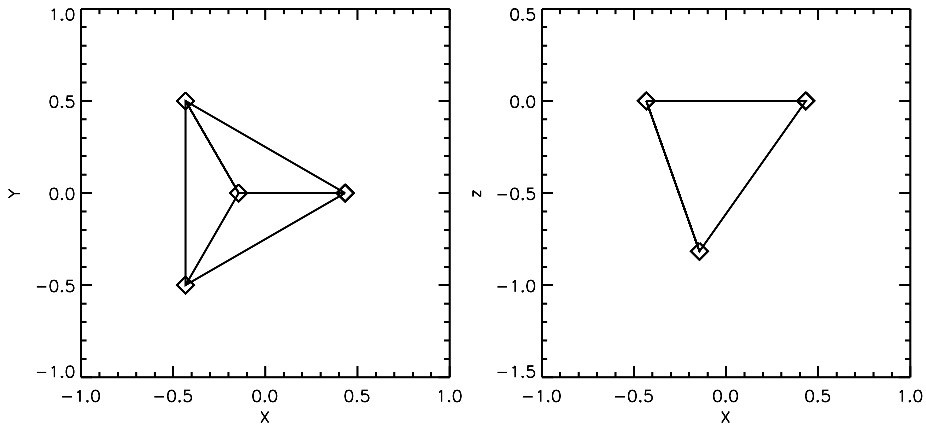

Figure 2: Plots of the locations of the test "spacecraft" in (a) the XY plane and (b) the XZ plane.

this plane (see Fig. 2). As such, throughout this study the current direction is always perpendicular to one plane of the spacecraft tetrahedron.

In order to examine the response of the curlometer technique to the model input current, $\nabla \times \mathbf{B}$ and $\nabla \cdot \mathbf{B}$ were calculated using the curlometer for currents centred in and around the spacecraft tetrahedron. $\nabla \times \mathbf{B}$ and $\nabla \cdot \mathbf{B}$ were calculated for a 100x100 grid of locations with a resolution of $0.02\ r_{sc} \times 0.02\ r_{sc}$ where r_{sc} is the spacecraft separation. To compare the results of the model curlometer with the known input current, the current flowing through the spacecraft tetrahedron was also calculated for each location of the current system centre. Given the form of the current, this is non-trivial. As a simplification, the current system was calculated in a 2-dimensional array with a resolution of $10^{-3}\sigma \times 10^{-3}\sigma$. The current flowing through the tetrahedron was estimated by summing the array elements that fall within the face of the tetrahedron perpendicular to the input current. It should be noted that the vector sum of the areas of the faces of the tetrahedron that are not perpendicular to the current is equivalent to the vector area of the face that is perpendicular to the current.

3. Model results

The limiting case of the model current system employed is an infinitely long, infinitely thin line current ($\sigma = 0$). In this case, the current density flowing through the tetrahedron can be calculated explicitly as the total current divided by the sum of the vector areas of three faces of the tetrahedron. Figure 3 shows the results from the curlometer technique for this current. The panels (a)-(d) show the current density (j) calculated by the curlometer scaled by π, $\nabla \cdot \mathbf{B}$ calculated by the curlometer, the ratio of the current density calculated by the curlometer to the input current density flowing through the tetrahedron (j/j_{in}), and $|\nabla \cdot \mathbf{B}/\nabla \times \mathbf{B}|$ respectively against position of the centre of the current system in the XY plane. The colours show the value of the various parameters calculated by the curlometer when the current was centred on that point. For all points within the tetrahedron, the input current density is constant. Panels (e) and (f) show histograms of j/j_{in} and $|\nabla \cdot \mathbf{B}/\nabla \times \mathbf{B}|$ for points within the tetrahedron.

Panel (c) shows that the curlometer tends to under-estimate the currents flowing through the tetrahedron, detecting approximately 20% of the input current density, although for currents located close to the spacecraft (at the vertices of the tetrahedron), the current density is over-estimated. This is due to the magnetic field becoming increasingly large close to the location of the current for this particular current system ($\mathbf{B} = \mu_0 j_0/2\pi r \to \infty$ as $r \to 0$). The area over which this over-estimation occurs is largest about the out-of-the-plane spacecraft. Panel (e) shows that both the modal current density (taken to be the peak of the histogram) and the mean current density were less than the input current density. The mean current is approximately 25% higher than the modal current due to the large current densities calculated when the currents lay close to a spacecraft.

Panel (a) shows that the curlometer calculates a curl of $\mathbf{B}$ for currents that lie outside the tetrahedron and thus it infers currents inside the tetrahedron, although these are small. The magnitude of j decays more slowly along the

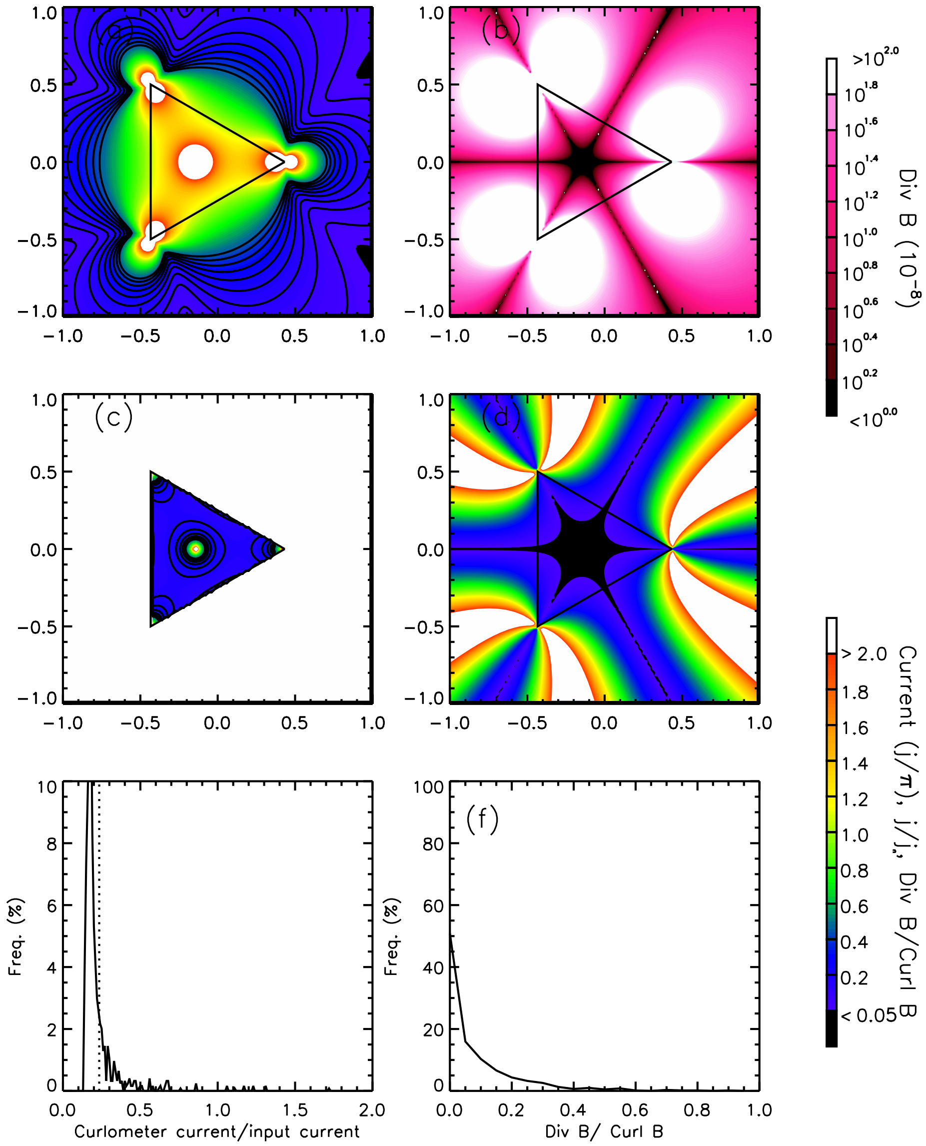

Figure 3: Plots of (a) j/π, (b) $\nabla \cdot \mathbf{B}$, (c) j/j_{in}, (d) $|\nabla \cdot \mathbf{B}/\nabla \times \mathbf{B}|$ for different locations of the input current. The input current is an infinitely long, infinitely thin line current. White (black) indicates large (small) values that are off the given scale. Panel (e) and (f) show a histograms of the j/j_{in} and $|\nabla \cdot \mathbf{B}/\nabla \times \mathbf{B}|$ within the tetrahedron. The dashed line in (e) shows the mean value of j/j_{in} for currents within the tetrahedron. (Colour figure for web only)

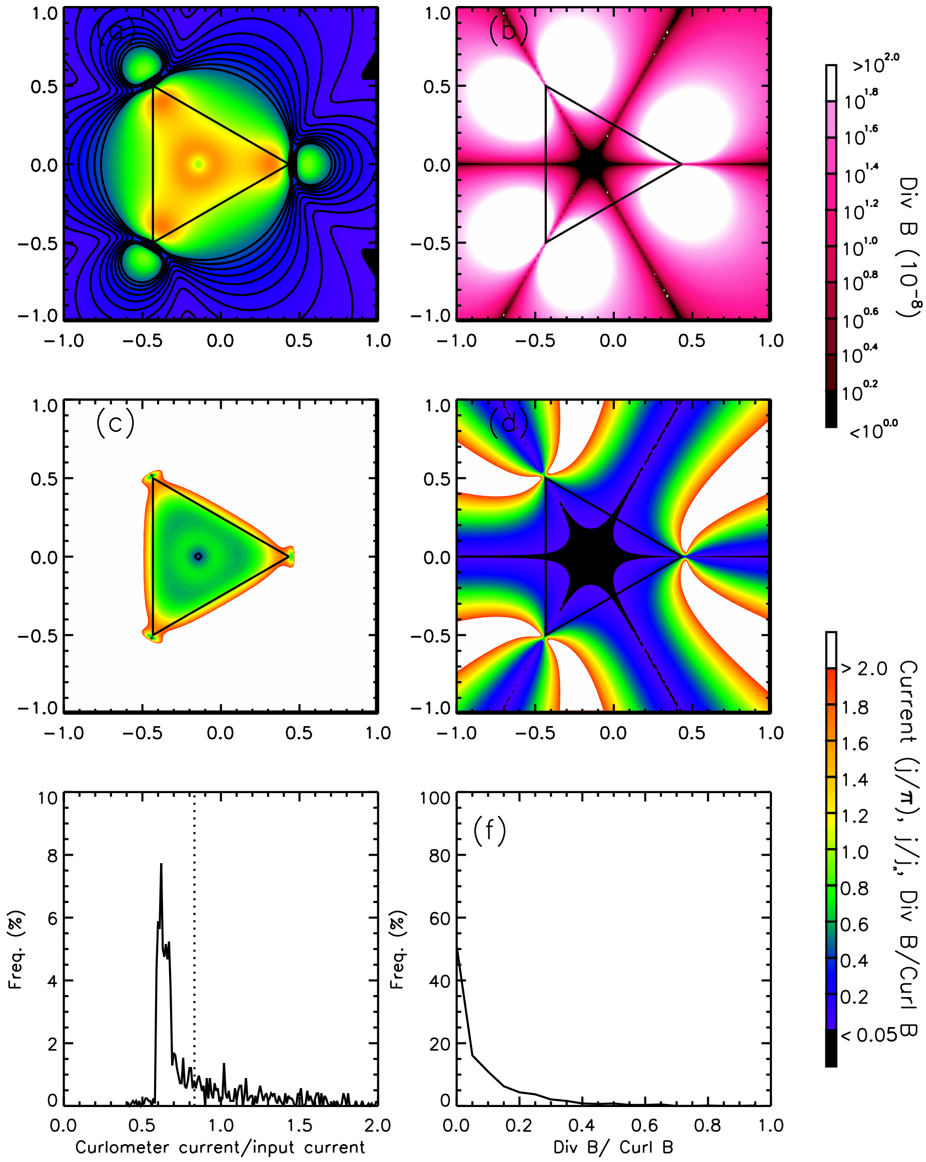

Figure 4: Plots of (a) j, (b) $\nabla \cdot \mathbf{B}$, (c) j/j_{in}, (d) $|\nabla \cdot \mathbf{B}/\nabla \times \mathbf{B}|$ for different locations of the input current. The input current is an infinitely long line current with a radial distribution of $j = e^{-r^2/\sigma^2}/2\ \hat{\mathbf{z}}$, where $\sigma = 0.1 r_{sc}$. Panel (e) and (f) show a histograms of the j/j_{in} and $|\nabla \cdot \mathbf{B}/\nabla \times \mathbf{B}|$ within the tetrahedron. (Colour figure for web only)

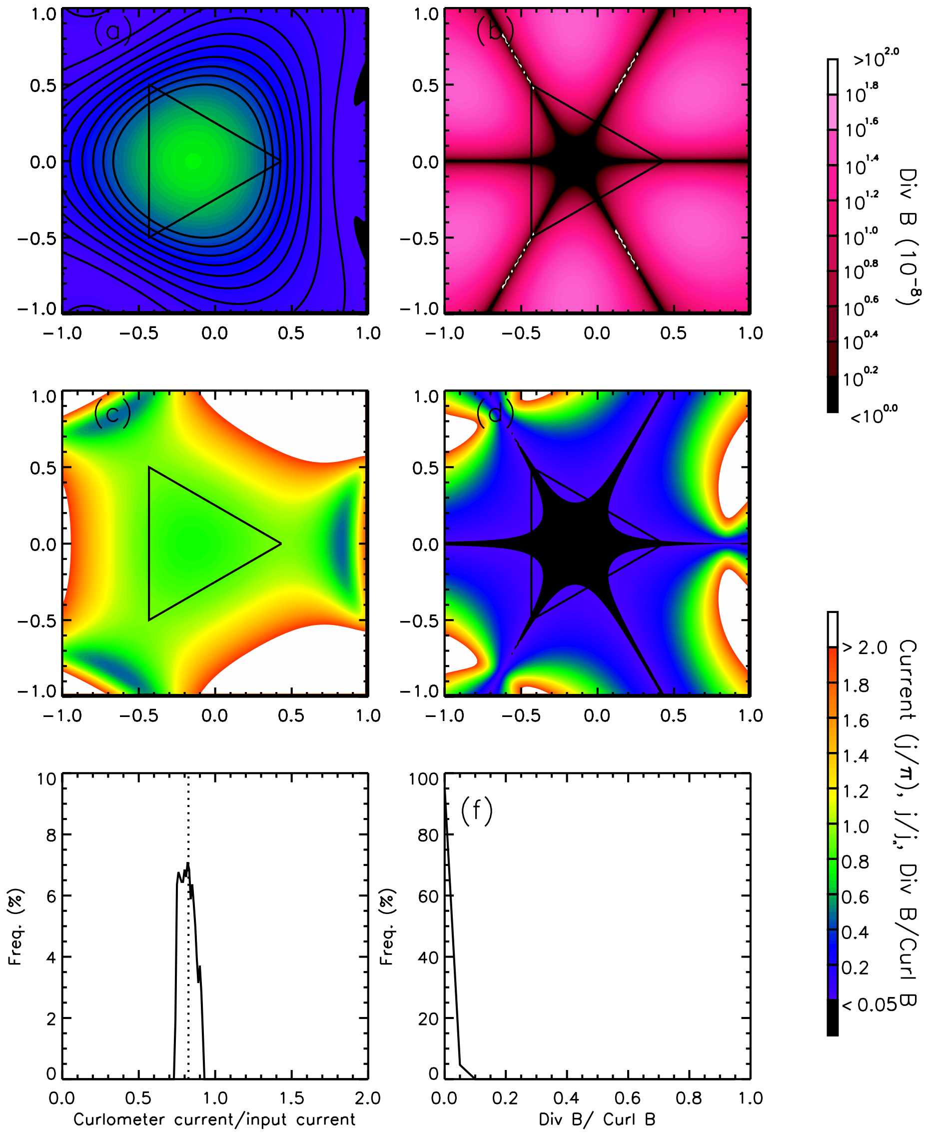

Figure 5: Plots of (a) j, (b) $\nabla \cdot \mathbf{B}$, (c) j/j_{in}, (d) $|\nabla \cdot \mathbf{B}/\nabla \times \mathbf{B}|$ for different locations of the input current. White (black) indicates large (small) values that are off the given scale. The input current is an infinitely long line current with a radial distribution of $j = e^{-r^2/\sigma^2}/2\ \hat{\mathbf{z}}$, where $\sigma = 0.5r_{sc}$. Panel (e) and (f) show a histograms of the j/j_{in} and $|\nabla \cdot \mathbf{B}/\nabla \times \mathbf{B}|$ within the tetrahedron. (Colour figure for web only)

perpendicular bisectors of the faces of the tetrahedron. Along these bisectors, $|\nabla\cdot\mathbf{B}/\nabla\times\mathbf{B}| < 0.4$, which is comparable with the limits used to indicate reliable curlometer results from spacecraft data for a current sheet (e.g. Runov et al., 2005), although is significantly higher than the values determined for currents passing through the tetrahedron ($|\nabla \cdot \mathbf{B}/\nabla \times \mathbf{B}| < 0.05$).

Figures 4 and 5 show similar plots to Fig. 3 for current systems with widths σ of 0.1 and 0.5 times the spacecraft separation respectively. Given that the current system has an extent in XY plane, j_{in} is calculated as the portion of the current system passing through the tetrahedron, as described in Section 2.

Comparing Fig. 4 with Fig. 3 shows that the peaks in j in the vicinity of the spacecraft are no longer present, replaced by local minima. This is because the magnetic field tends to infinity close to the infinitely thin line current, whereas the magnetic field is zero at the centre of a distributed current system (Eq. 1). Panels (c) and (e) show that $j/j_{in} \approx 0.6$ within the tetrahedron and that there is variation in j/j_{in} across the tetrahedron. Panel (c) shows that the largest j/j_{in} are along the edges of the tetrahedron and (to a lesser extent) in a ring around the out-of-the-plane spacecraft.

Comparing Fig. 5 with Fig. 4 shows that the variations of j/j_{in} within the tetrahedron are reduced for larger current systems (Panel c). In particular, the high j/j_{in} tail has been removed such that there are no points with $j/j_{in} > 1$ within the tetrahedron. Panel (e) shows that the mean j/j_{in} (dotted line) is close to the peak of the distribution for the $\sigma = 0.5$ case. Comparing Panel (d) between Figs. 5 and 3 shows that $|\nabla \cdot \mathbf{B}/\nabla \times \mathbf{B}|$ has similar pattern in both figures, suggesting that the pattern for $|\nabla \cdot \mathbf{B}/\nabla \times \mathbf{B}|$ is scalable.

For currents centred outside the tetrahedron, the curlometer is able to estimate the current density of the portion of the current flowing through the tetrahedron. Panel (c) shows that when a current centre is less than $\sigma/2$ from one of the faces of the tetrahedron, the curlometer results are comparable to those from currents passing through the tetrahedron. With increasing distance from the tetrahedron, the curlometer over-estimates the current density, as in the line current case. It is interesting to note, however, that close to the vertices of the tetrahedron, but for currents centred outside the tetrahedron, there are small regions in which the current passing through the tetrahedron is underestimated.

Figure 6 shows the variation of j/j_{in} and $|\nabla\cdot\mathbf{B}/\nabla\times\mathbf{B}|$ with the width of the current system relative to the spacecraft separation. The black lines indicate the mean value within the tetrahedron. The red line in panel (a) shows the modal value (taken to be the peak of a histogram of the current density with a bin size of 0.01). The error bars indicate the standard deviation.

As the current system width increases relative to the separation of the spacecraft, the curlometer tends to return current densities closer to the input current density flowing through the tetrahedron. The modal and mean current densities converge such that above $\sigma/r_{sc} = 0.6$ they are approximately equal and the standard deviation decreases. Whilst the modal value of j/j_{in} increases fairly steadily with σ/r_{sc}, the mean current densities show a decrease between $\sigma/r_{sc} = 0.1$ and $\sigma/r_{sc} = 0.3$. The mean value of $|\nabla\cdot\mathbf{B}/\nabla\times\mathbf{B}|$ decreases steadily with σ/r_{sc}.

Below $\sigma/r_{sc} = 0.5$, both the mean and modal j/j_{in} show deviation away from the smooth curve evident above $\sigma/r_{sc} = 0.5$. We suggest that this deviation is due to the limitations of estimating the input current density from a finite resolution square grid across a triangular face of the tetrahedron. This is supported by the fact that $|\nabla\cdot\mathbf{B}/\nabla\times\mathbf{B}|$, which is determined from the explicitly calculated magnetic field, varies smoothly with σ/r_{sc}. Note, however, that the values for $\sigma/r_{sc} = 0$ are explicitly calculated and therefore not subject to this error.

4. Summary and Discussion

In the previous section we have shown that the results from the curlometer technique can vary with respect to position and width of a line current relative to the observing spacecraft tetrahedron. For the model line current examined, the results show:

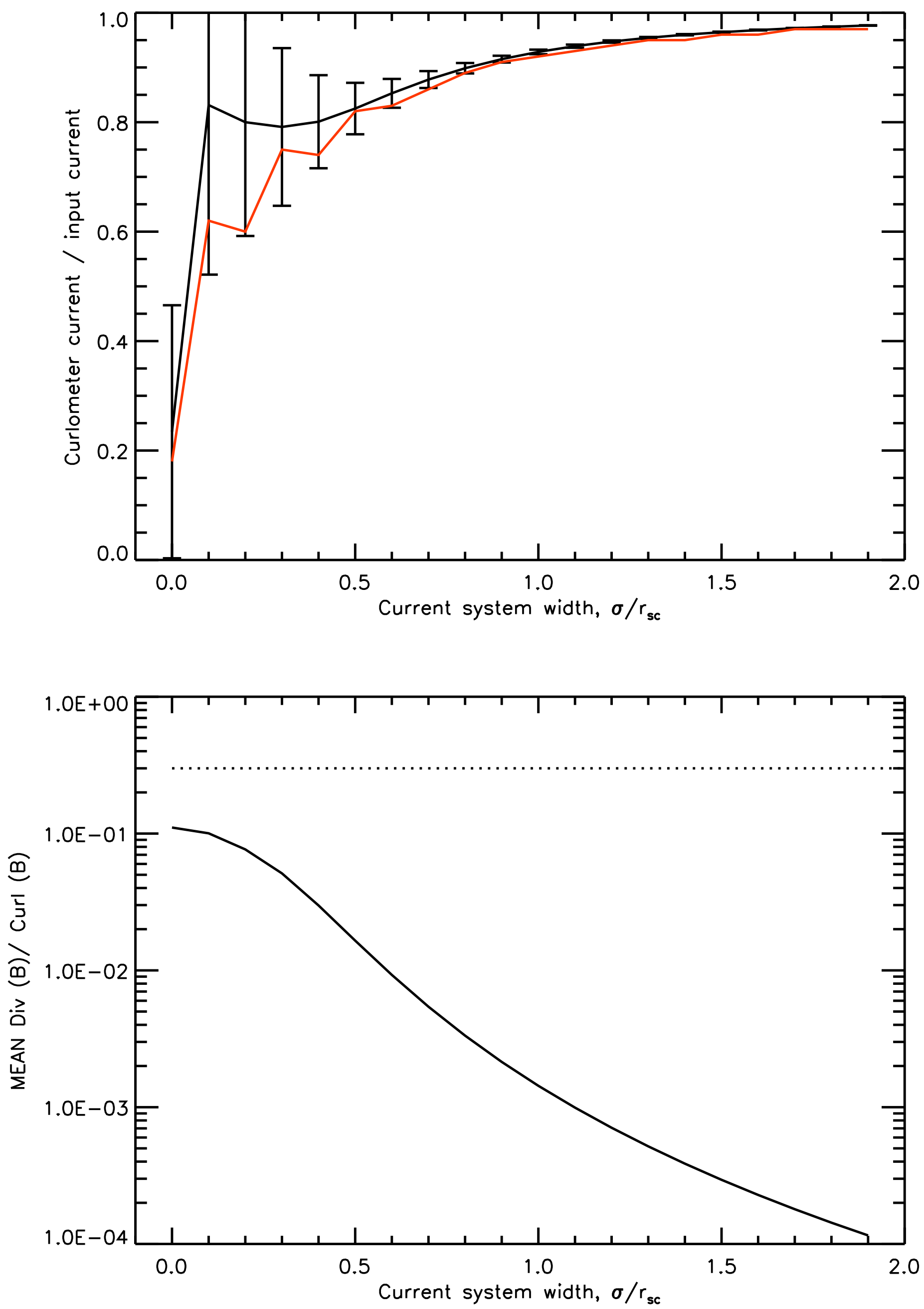

Figure 6: Plots of (a) mean (black) and modal (red) j/j_in and (b) $|\nabla \cdot \mathbf{B}/\nabla \times \mathbf{B}|$ against current system width for currents systems with their centre passing through the spacecraft tetrahedron. (Colour figure for web only)

1. In the limit of an infinitely thin, infinitely long line current, the curlometer tends to return 20% of the current density on average, but the value returned is strongly dependant on the position of the current within the tetrahedron,
2. The curlometer tends to under-estimate the current density for currents flowing through the tetrahedron, although this under-estimation reduces as line current width increases,
3. The curlometer detects the effects of currents centred outside the tetrahedron. For those line currents which are less than $\sigma/2$ from the edge of the the tetrahedron, j/j_{in} is comparable to those currents with centres within the tetrahedron. Outside of this, the curlometer over-estimates the current flowing through the tetrahedron.
4. $|\nabla \cdot \mathbf{B}/\nabla \times \mathbf{B}|$ is small (< 0.1) for currents passing through the tetrahedron and is larger for currents passing outside the tetrahedron, although along the perpendicular bisector of the faces of the tetrahedron, $|\nabla \cdot \mathbf{B}/\nabla \times \mathbf{B}|$ remains relatively low,

In this section we discuss these results in the context of multi-scale, multi-spacecraft missions and previous results.

In the model used, there were no uncertainties in the position of the observing spacecraft and the magnetic field values. As such, the non-zero calculation of $\nabla\cdot\mathbf{B}$ is due to non-linear variations of the magnetic field. For the current systems tested, $|\nabla \cdot \mathbf{B}/\nabla \times \mathbf{B}|$ was significantly less than values typically calculated from Cluster data (e.g. Forsyth et al., 2008) and from the model results of Runov et al. (2005). We suggest that the higher values of $|\nabla \cdot \mathbf{B}/\nabla \times \mathbf{B}|$ often calculated from Cluster data are indicative of uncertainties in the spacecraft positions and magnetic field values, although are also dependant on the form of the current being examined. As previously discussed by Robert et al. (1998), there is not necessarily a dependence between the uncertainties in the diagonal and off-diagonal terms in the $\nabla\mathbf{B}$ dyad, although we note that both the error in the current returned by the curlometer and $|\nabla \cdot \mathbf{B}/\nabla \times \mathbf{B}|$ decreased with increasing current system width. One must be aware that for a multi-scale, multi-tetrahedra mission, the factors that determine $|\nabla \cdot \mathbf{B}/\nabla \times \mathbf{B}|$ will vary between the scale sizes (non-linearity will be more important than uncertainties in position at large scale sizes and vice-versa). One must also be aware that the results presented here are valid for the current system tested but are current system dependant (see e.g. Runov et al., 2005)

Figure 6 shows that as the scale size of the current increases, the mean value of $|\nabla \cdot \mathbf{B}/\nabla \times \mathbf{B}|$ for currents passing through the tetrahedron becomes increasingly small. Previous studies have used $|\nabla \cdot \mathbf{B}/\nabla \times \mathbf{B}|$ to determine the quality of the results from the curlometer, with lower values indicating more reliable results, despite pre-Cluster studies suggesting that $\nabla \cdot \mathbf{B}$ is not a reliable indicator of quality (Robert and Roux, 1993; Dunlop and Balogh, 1993; Coeur-Joly et al., 1995; Robert et al., 1995, 1998). However, one must consider that alternative indicators of quality rely on a priori knowledge of the current system being investigated or do not consider local variations in the magnetic field. As such, comparing model current systems and spacecraft data is increasingly important for multi-scale missions.

Comparing the width of the line currents relative to the separation of the spacecraft (σ/r_{sc}) and the proportion of the input current returned gives an indication that one can set a lower limit to the relative width of the line current to the spacecraft separation for which the curlometer provides meaningful results. For line currents with a $\sigma/r_{sc} \geq 0.5$ the curlometer detects approximately $80 \pm 15\%$ of the input current. In terms of multi-tetrahedra missions, this indicates that one must take care when comparing currents from various scale sizes of tetrahedron and that one can set limits on the required accuracy of the curlometer such that the results from larger tetrahedra can be disregarded for current systems below a given relative scale size.

Clearly, in order to use the curlometer technique for a multi-tetrahedron spacecraft mission, one must be aware that the location of the current system under investigation within the tetrahedra could have a significant effect on the results returned by the various tetrahedra, especially if the current system is small compared to one or more of the spacecraft tetrahedra. One would expect that, for most situations, the smallest tetrahedra will give the most accurate results and the largest the least accurate, although this does not take into account uncertainties in the measurement of spacecraft position and magnetic field, the effect of which is likely to be greater for smaller tetrahedra rather than larger ones.

The majority of previous studies into the accuracy and response of the curlometer have concentrated on current sheets, either of the Harris type or intrinsic to global magnetic field models. However, Robert et al. (1998) used simple current tube models (line currents) to examine how the results of the curlometer varied with varying tetrahedron shape in order to determine a parameter of the tetrahedron shape that could be used as an indicator of quality for the current density measurements. In their study the barycentre of the tetrahedra were at a fixed location and the tetrahedra were normalised to have the same mean spacecraft separation and hence no attempt was made to examine the effect of the location or width of the line current on the curlometer.

It is not clear that the effects of variations in the tetrahedron shape and size on the results of the curlometer for line and planar currents are directly comparable. It is expected that the curlometer will return more accurate results when the current systems is much larger than the spacecraft tetrahedron as variations in the field can be better approximated as linear. For the same reason, variations in the shape of the tetrahedron are also expected to cause variations in the curlometer results. Studies have shown that this is true for planar current systems (Robert and Roux, 1993; Dunlop and Balogh, 1993; Coeur-Joly et al., 1995; Robert et al., 1995) , but there has previously been no direct comparison between the results for line currents and planar currents. However, by comparing our results with the results of Runov et al. (2005), it can be seen that $|\nabla \cdot \mathbf{B}/\nabla \times \mathbf{B}|$ is much smaller in the case of a line current and appears to drop continuously with increasing current system width, whereas $|\nabla \cdot \mathbf{B}/\nabla \times \mathbf{B}|$ tends towards ≈ 0.28 for the current sheet case. Also, the relative errors of the currents appear to tend towards similar values for both line and planar current systems larger than the spacecraft separation.

Given that accuracy of the curlometer is dependant not only on the relative size and shape of the spacecraft tetrahedron but also on the current system under observation, it is useful to determine whether or not the observed current system is similar to a planar or line current structure. These two current systems should be discernible from the magnetic field data. For a planar current system, the magnetic field rotates in one direction, the direction perpendicular to the current and the current sheet normal. In the line current case, the magnetic field parallel to the current direction is invariant such that the field varies in the plane perpendicular to the current. It should be noted that in order to determine if the field is invariant in the direction perpendicular or parallel to the current direction requires accurate determination of the current direction, an issue which we do not address in this paper.

Although the results presented are specific to the line currents tested, they clearly show that in order to compare results from the curlometer across various scale sizes one has to take into account the scale sizes being examined and the location of the current system. This is clearly a non-trivial task. We suggest, however, that by comparing the curlometer results from multiple scales with a model of the current system under examination may prove insightful in most cases.

5. Conclusions

The results of the curlometer technique have been examined for an infinitely long line current with a given radial distribution of current density for a range of positions relative to the observing spacecraft tetrahedron and for a range of scale sizes (i.e. line current widths) of the radial variation of the current density. The magnetic field associated with these current systems was explicitly calculated at the locations of four test "spacecraft", and these data were then processed using the curlometer technique. The results show:

1. For small-scale line currents, the proportion of the input current returned by the curlometer varies with the location of the centre of the current system

through the spacecraft tetrahedron,

2. For small-scale line currents, the curlometer under-estimates the current density by up to 80%, although for current systems with $\sigma/r_{sc} \geq 0.5$, the curlometer tends to return 80% of the current,
3. The curlometer will detect the effects of currents located entirely outside the limits of the spacecraft tetrahedron, although these values are small compared to the input current,
4. $|\nabla \cdot \mathbf{B}/\nabla \times \mathbf{B}|$ can be low for currents detected outside the spacecraft tetrahedron and as such, is not always a useful indicator of the quality of the determination of j.

The results presented here are specific to the line currents examined, although our results suggest that in order to meaningfully compare the results from the curlometer at various scale sizes, one should compare spacecraft data with a model of the current system under examination.

6. Acknowledgements

CF, ANF, CJO and APW were supported by STFC grant PP/E001173/1. ML was supported by STFC grant PP/E000983.

References

Coeur-Joly, O., Robert, P., Chanteur, G., Roux, A., 1995. Simulated daily summaries of cluster four-point magnetic field measurements. In: Proceedings of Cluster Workshops, Braunschweig, 28-30 Sep. 1994, Toulouse, 16-17 Nov. 1994. European Space Agency, Paris, France, pp. 223–227.

Dunlop, M. W., Balogh, A., 1993. On the analysis and interpretation of four spacecraft magnetic field measurements in terms of small scale plasma processes. In: Proc. International. Conf. "Spatio-Temporal Analysis for Resolving plasma Turbulence (START)", Aussois, 31 Jan.-5 Feb. 1993. European Space Agency, Paris, France, pp. 289–293.

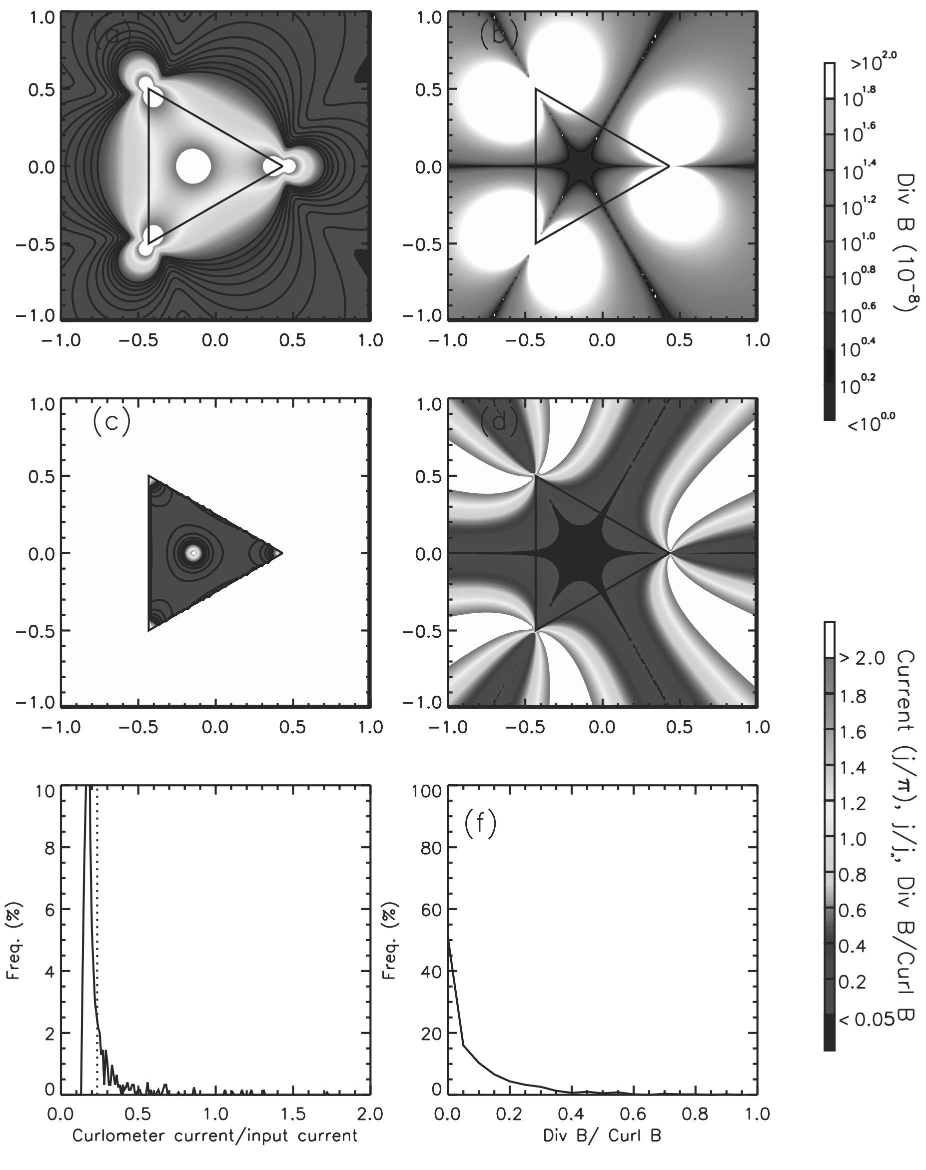

Figure 7: Plots of (a) j/π, (b) $\nabla \cdot \mathbf{B}$, (c) j/j_{in}, (d) $|\nabla \cdot \mathbf{B}/\nabla \times \mathbf{B}|$ for different locations of the input current. The input current is an infinitely long, infinitely thin line current. White (black) indicates large (small) values that are off the given scale. Panel (e) and (f) show a histograms of the j/j_{in} and $|\nabla \cdot \mathbf{B}/\nabla \times \mathbf{B}|$ within the tetrahedron. The dashed line in (e) shows the mean value of j/j_{in} for currents within the tetrahedron. (Print copy figure)

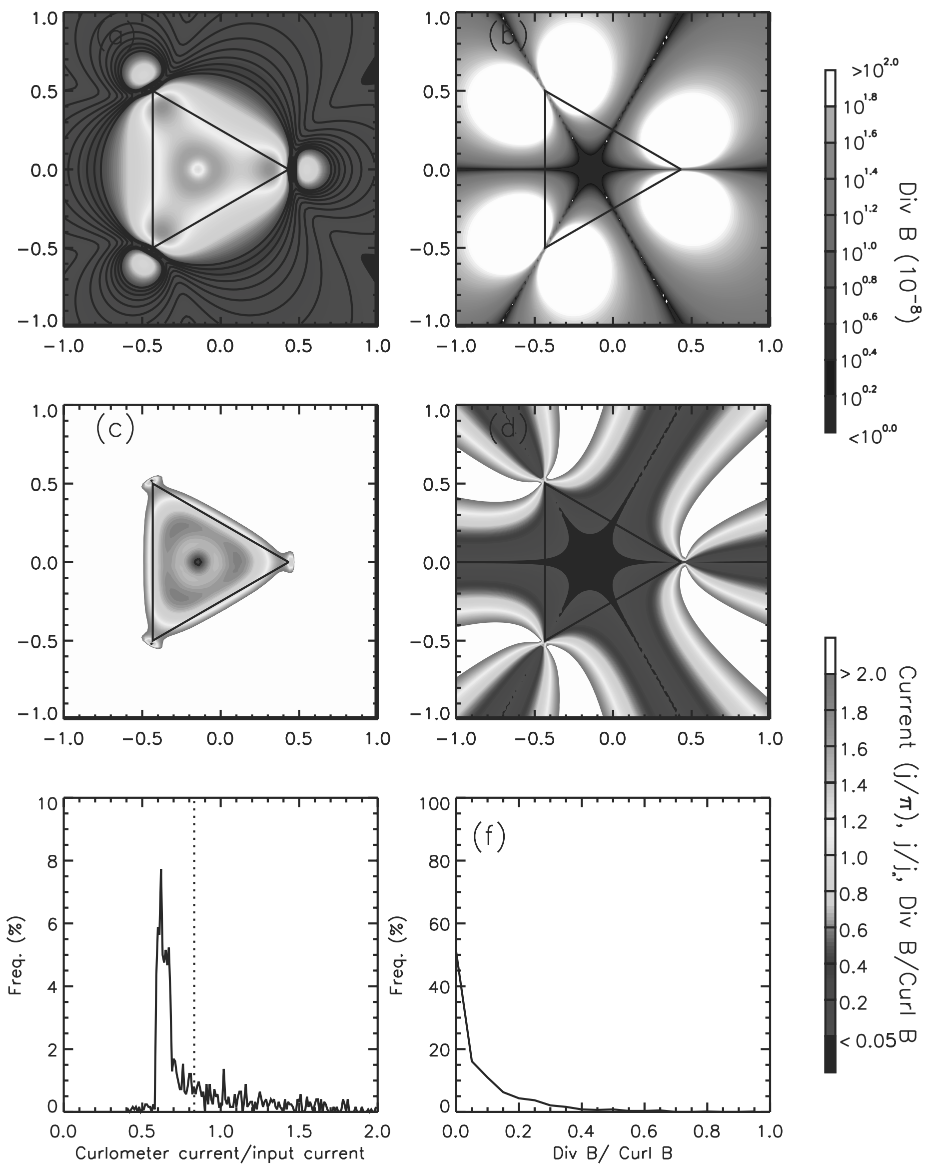

Figure 8: Plots of (a) j, (b) $\nabla \cdot \mathbf{B}$, (c) j/j_{in}, (d) $|\nabla \cdot \mathbf{B}/\nabla \times \mathbf{B}|$ for different locations of the input current. The input current is an infinitely long line current with a radial distribution of $j = e^{-r^2/\sigma^2}/2\ \hat{\mathbf{z}}$, where $\sigma = 0.1 r_{sc}$. Panel (e) and (f) show a histograms of the j/j_{in} and $|\nabla \cdot \mathbf{B}/\nabla \times \mathbf{B}|$ within the tetrahedron. (Print copy figure)

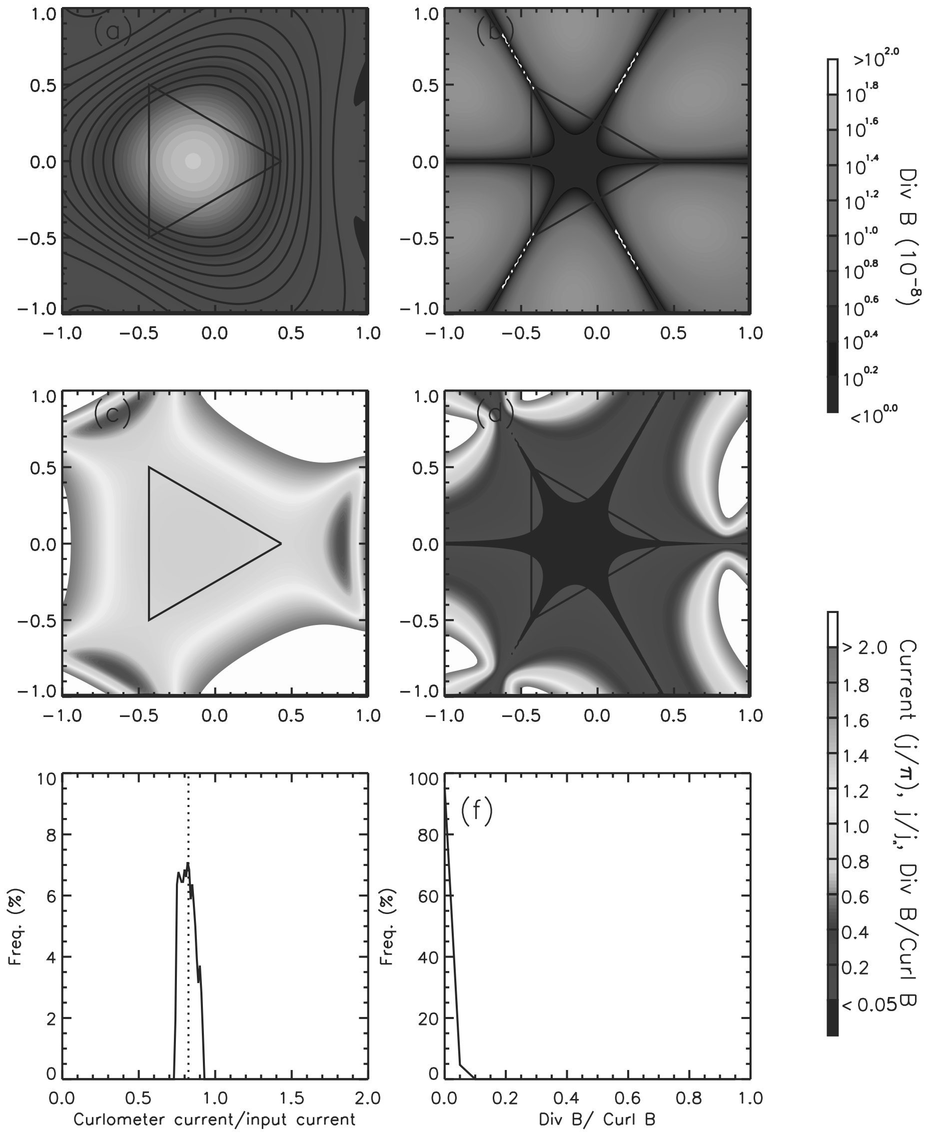

Figure 9: Plots of (a) j, (b) $\nabla \cdot \mathbf{B}$, (c) j/j_{in}, (d) $|\nabla \cdot \mathbf{B}/\nabla \times \mathbf{B}|$ for different locations of the input current. White (black) indicates large (small) values that are off the given scale. The input current is an infinitely long line current with a radial distribution of $j = e^{-r^2/\sigma^2}/2\ \hat{\mathbf{z}}$, where $\sigma = 0.5r_{sc}$. Panel (e) and (f) show a histograms of the j/j_{in} and $|\nabla \cdot \mathbf{B}/\nabla \times \mathbf{B}|$ within the tetrahedron. (Print copy figure)

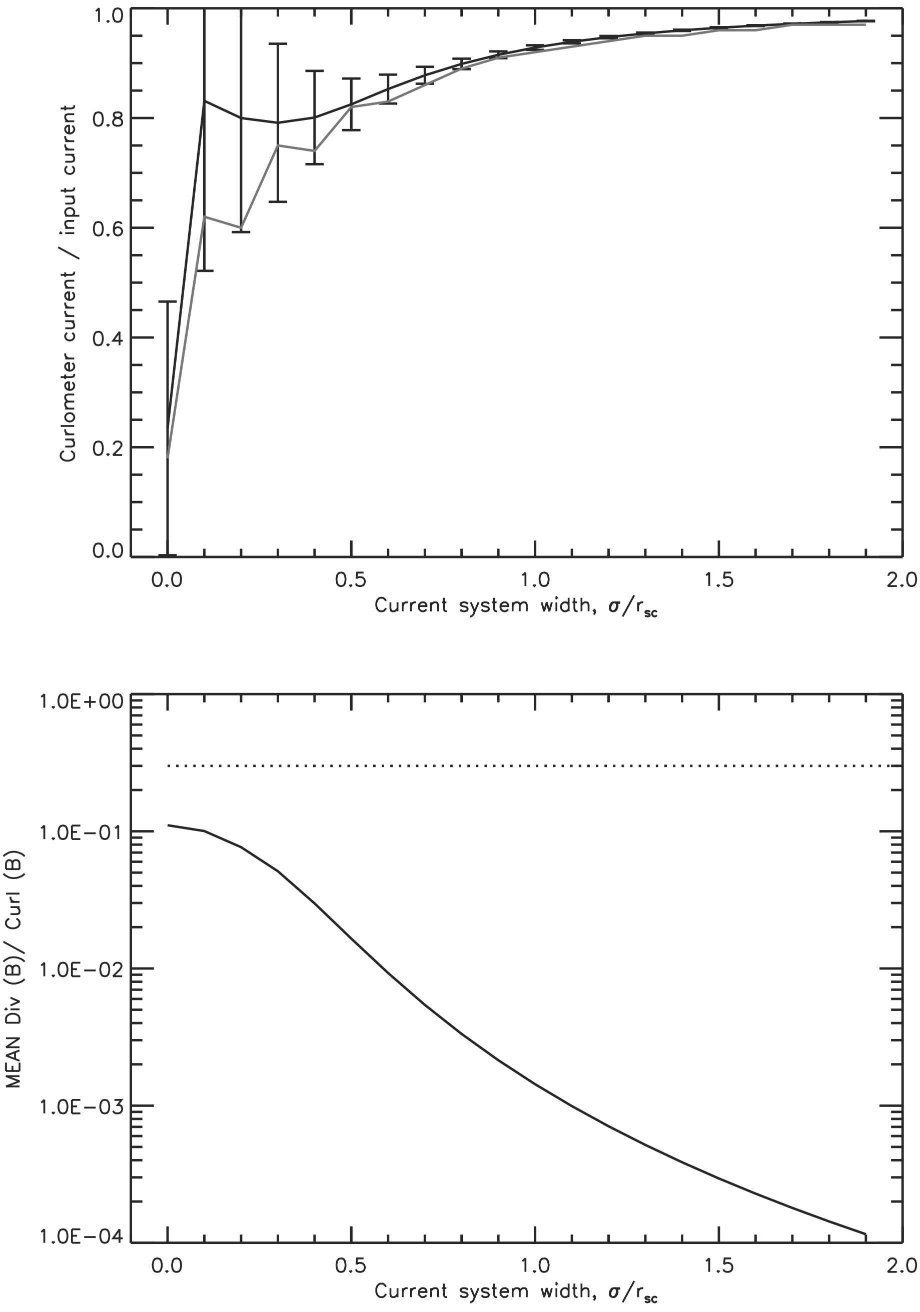

Figure 10: Plots of (a) mean (black) and modal (red) j/j_in and (b) $|\nabla \cdot \mathbf{B}/\nabla \times \mathbf{B}|$ against current system width for currents systems with their centre passing through the spacecraft tetrahedron. (Print copy figure)

Dunlop, M. W., Balogh, A., Mar. 2005. Magnetopause current as seen by Cluster. Ann. Geophys. 23, 901–907.

Dunlop, M. W., Balogh, A., Glassmeier, K.-H., Robert, P., Nov. 2002. Four-point Cluster application of magnetic field analysis tools: The Curlometer. J. Geophys. Res. 107, A01384.

Dunlop, M. W., Eastwood, J. P., 2008. The curlometer and other gradient based methods. In: Paschmann, G., Daly, P. W. (Eds.), Multi-Spacecraft Analysis Methods Revisited. ISSI, pp. 17–25.

Dunlop, M. W., Southwood, D. J., Glassmeier, K.-H., Neubauer, F. M., 1988. Analysis of multipoint magnetometer data. Adv. Space Res. 8, 273–277.

Forsyth, C., Lester, M., Cowley, S. W. H., Dandouras, I., Fazakerley, A. N., Fear, R. C., Frey, H. U., Grocott, A., Kadokura, A., Lucek, E., Rème, H., Milan, S. E., Watermann, J., Feb. 2008. Observed tail current systems associated with bursty bulk flows and auroral streamers during a period of multiple substorms. Ann. Geophys. 26, 167–184.

Harris, E. G., 1962. On a plasma sheet separating regions of oppositly directed magnetic field. Nuovo Cimento 23, 151–121.

Henderson, P. D., Owen, C. J., Lahiff, A. D., Alexeev, I. V., Fazakerley, A. N., Lucek, E., Rème, H., Nov. 2006. Cluster PEACE observations of electron pressure tensor divergence in the magnetotail. Geophys. Res. Lett. 33, L22106.

Henderson, P. D., Owen, C. J., Lahiff, A. D., Alexeev, I. V., Fazakerley, A. N., Yin, L., Walsh, A. P., Lucek, E., Réme, H., May 2008. The relationship between $j \times B$ and $\nabla . P_e$ in the magnetotail plasma sheet: Cluster observations. J. Geophys. Res. 113, A07S31.

Phan, T., Dunlop, M., Paschmann, G., Klecker, B., Bosqued, J., Rème, H., Balogh, A., Twitty, C., Mozer, F., Carlson, C., Mouikis, C., Kistler, L., Jul. 2004. Cluster observations of continuous reconnection at the magnetopause under steady interplanetary magnetic field conditions. Ann. Geophys. 22, 2355–2367.

Robert, P., Dunlop, M. W., Roux, A., Chanteur, G., 1998. Accuracy of current density determination. In: Paschmann, G., Daly, P. W. (Eds.), Analysis Methods for Multi-Spacecraft Data. ISSI, pp. 395–418.

Robert, P., Roux, A., 1993. Influence of the shape of the tetrahedron on the accuracy of the estimation of the current density. In: Proc. International. Conf. "Spatio-Temporal Analysis for Resolving plasma Turbulence (START)", Aussois, 31 Jan.-5 Feb. 1993. European Space Agency, Paris, France, pp. 289–293.

Robert, P., Roux, A., Coeur-Joly, O., 1995. Validity of the estimate of the current density along cluster orbit with simulated magnetic data. In: Proceedings of Cluster Workshops, Braunschweig, 28-30 Sep. 1994, Toulouse, 16-17 Nov. 1994. European Space Agency, Paris, France, pp. 229–233.

Runov, A., Nakamura, R., Baumjohann, W., Zhang, T. L., Volwerk, M., Eichelberger, H.-U., Balogh, A., Jan. 2003. Cluster observation of a bifurcated current sheet. Geophys. Res. Lett. 30, 8–1.

Runov, A., Sergeev, V. A., Baumjohann, W., Nakamura, R., Apatenkov, S., Asano, Y., Volwerk, M., Vörös, Z., Zhang, T. L., Petrukovich, A., Balogh, A., Sauvaud, J.-A., Klecker, B., Rème, H., Jun. 2005. Electric current and magnetic field geometry in flapping magnetotail current sheets. Ann. Geophys. 23, 1391–1403.

Runov, A., Sergeev, V. A., Nakamura, R., Baumjohann, W., Apatenkov, S., Asano, Y., Takada, T., Volwerk, M., Vörös, Z., Zhang, T. L., Sauvaud, J.-A., Rème, H., Balogh, A., Mar. 2006. Local structure of the magnetotail current sheet: 2001 Cluster observations. Ann. Geophys. 24, 247–262.

Tsyganenko, N. A., Nov. 1987. Global quantitative models of the geomagnetic field in the cislunar magnetosphere for different disturbance levels. Planet. Sp. Sci. 35, 1347–1358.